Published in final edited form as:
*Sci Transl Med*. 2013 July 3; 5(192): 192ra87. doi:10.1126/scitranslmed.3005958.

# TCR-ligand $k_{off}$-rate predicts protective capacity of antigen-specific CD8+ T cells for adoptive transfer

**Magdalena Nauerth**[1,*], **Bianca Weißbrich**[1,*], **Robert Knall**[1,*], **Tobias Franz**[1], **Georg Dössinger**[1], **Jeannette Bet**[1,2], **Paulina J. Paszkiewicz**[1,2], **Lukas Pfeifer**[1], **Mario Bunse**[3,4], **Wolfgang Uckert**[3,4], **Rafaela Holtappels**[5], **Dorothea Gillert-Marien**[5], **Michael Neuenhahn**[1,6,7], **Angela Krackhardt**[6,8], **Matthias J. Reddehase**[5,9], **Stanley R. Riddell**[2,10,11], and **Dirk H. Busch**[1,2,6,7]

[1]Institute for Medical Microbiology, Immunology and Hygiene, Technische Universität München, Munich, Germany

[2]Focus Group “Clinical Cell Processing and Purification”, Institute for Advanced Study, Technische Universität München, Munich, Germany

[3]Max Delbrück Center for Molecular Medicine, Berlin, Germany

[4]Humboldt-Universität Berlin, Berlin, Germany

[5]Institute for Virology and Research Center for Immunology (FZI), University Medical Center of the Johannes Gutenberg-University, Mainz, Germany

[6]Clinical Cooperation Groups ‘‘Antigen-specific Immunotherapy’’ and “Immune Monitoring”, Helmholtz Center Munich (Neuherberg) and Technische Universität München, Munich, Germany

[7]DZIF - National Centre for Infection Research, Munich, Germany

[8]Medical Department III, Hematology and Oncology, Technische Universität München, Munich, Germany

[9]Helmholtz Virtual Institute on Viral Strategies of Immune Evasion (VISTRIE), Helmholtz Centre for Infection Research, Braunschweig, Germany

[10]Program in Immunology, Clinical Research Division, Fred Hutchinson Cancer Research Center, Seattle, Washington, USA

[11]Department of Medicine, University of Washington, Seattle, Washington, USA

Correspondence and requests for material should be addressed to: Dirk H. Busch Institute for Medical Microbiology, Immunology and Hygiene Technische Universität München, Trogerstrasse 30, 81675 Munich, Germany dirk.busch@mikrobio.med.tum.de phone: +49 (0) 89 4140 4120 fax: +49 (0) 89 4140 4131.

*These authors contributed equally to this work.

**Author Contributions**.

M.N., B.W., R.K., G.D., L.P., T.F., D.G.-M., M.B. and R.H. did experiments; J.B., P.J.P., M.N., R.H. and S.R.R. supplied cells; S.R.R. helped with the cell culture of human CMV specific T cell clones.; A.K. supplied blocking antibody and helped with the cell culture of human T cells; M.B. and W.U. supplied retroviral vectors and cells; D.H.B. conceived the study; R.K., M.N., and B.W. analyzed the data; M.J.R. designed the MCMV protection experiments and D.H.B. planned most experiments and supervised the study. M.N., B.W. and D.H.B. wrote the paper.

**Competing Financial Interests.**

The authors declare no competing financial interests.

## Abstract

Adoptive immunotherapy is a promising therapeutic approach for the treatment of chronic infections and cancer. Thereby, T cells within a certain range of high avidity for their cognate ligand are believed to be most effective. T cell receptor (TCR) transfer experiments indicate that a major part of avidity is hard-wired within the structure of the TCR. Unfortunately, rapid measurement of structural avidity of TCRs is difficult on living T cells. We developed a technology, where dissociation ($k_{off}$-rate) of truly monomeric peptide major histocompatibility complex (pMHC) molecules bound to surface expressed TCRs can be monitored by real-time microscopy in a highly reliable manner. A first evaluation of this method on distinct human Cytomegalovirus (CMV) -specific T cell populations revealed unexpected differences in the $k_{off}$-rates. CMV-specific T cells are currently being evaluated in clinical trials for efficacy in adoptive immunotherapy; therefore, determination of $k_{off}$-rates could guide selection of the most effective donor cells. Indeed, in two different murine infection models, we demonstrate that T cell populations with lower $k_{off}$-rates confer significantly better protection than populations with fast $k_{off}$-rates. These data indicate that $k_{off}$-rate measurements can improve the predictability of adoptive immunotherapy and provide diagnostic information on the *in vivo* quality of T cells.


## Introduction

Adoptive transfer of antigen-specific $CD8^+$ T cells is a promising approach for the treatment of viral infections (1, 2) and malignancies (3-5). Effective immunotherapy is believed to be dependent on T cell receptors (TCRs) within a range of high avidities for their cognate peptide-epitope major histocompatibility complex (pMHC) ligands. It has been shown that T cells expressing high avidity TCRs confer superior efficacy towards their target cells *in vitro* and *in vivo* (6-8) by recognizing their target cells earlier and faster in comparison to low avidity T cells (6). Thus, interrogating the avidity of T cells used for adoptive transfer or elicited by vaccines might provide important information on the efficacy of immune based therapies.

TCR avidity is mainly defined by functional readouts such as cytokine production after antigen-specific stimulation or lysis of target cells pulsed with limiting concentrations of peptide (“functional avidity”). The results of these assays can be influenced by many factors including the expression level of TCRs, adhesion molecules or co-receptors, and changes in components of the signaling cascade. Remarkably, not only the specificity for target antigens (9-11), but also functional avidity characteristics of specific TCRs could be transferred to newly generated T cells by transgenic expression (12, 13), indicating that the TCR structure is a major determinant of the binding avidity and T cell functionality. TCR gene transfer greatly facilitates clinical applications of adoptive T cell therapy, therefore it is of growing interest to analyze the ‘structural avidity’ that is defined by the affinity of the TCR to pMHC molecules combined with co-receptor binding via CD8 or CD4 of surface expressed TCRs.

Most attempts to determine structural TCR binding strength have been performed with surface plasmon resonance (SPR), where pMHCs and TCRs need to be provided as highly purified proteins. Since the expression of correctly folded TCRs is technically challenging,

SPR is difficult to use for analysis of a broader spectrum of TCRs. Alternative methods to examine the binding strength between TCR and pMHC are based on pMHC multimer binding and dissociation (14, 15). However, pMHC multimer staining intensity does not necessarily correlate with TCR binding avidity, and current pMHC-multimer dissociation assays monitor the dissociation of a multimeric complex, but do not allow accurate analysis of the binding strength between monomeric pMHCs and the TCR. Furthermore, these assays are prone to variability in the degree of pMHC multimerization and in the nature and concentration of blocking reagent, which is used to prevent rebinding of dissociated pMHCs to the TCRs (16).

Based on reversible multimers, so called *Strep*tamers (17), we developed a novel assay that circumvents the limitations of prior methods and allows the accurate determination of the dissociation of monomeric pMHCs from the TCRs on living T cells. Thereby, the dissociation kinetic is fully independent of the level of multimerization or the nature of a blocking reagent. Using this $k_{off}$-rate assay we demonstrate that T cell populations relevant for T cell therapy have highly variable $k_{off}$-rates. Furthermore, *in vivo* experiments using preclinical mouse models for infections demonstrated a strong correlation between the $k_{off}$-rate and protective capacity of transferred T cells.

## Results

### Development of a novel Streptamer-based $k_{off}$-rate assay

Multimeric pMHC dissociation experiments are currently used as a kind of “gold standard” to assess the structural avidity of antigen-specific T cells (Supplementary Figure 1A). Unfortunately, it is difficult to standardize this assay. For example, pMHC multimer dissociation kinetics strongly depend on the nature and the concentration of blocking reagents used to prevent rebinding of dissociated MHCs to TCRs (16). In addition, the kinetics of pMHC multimer dissociation experiments are very slow, in the range of minutes to hours. When working at low temperatures (4°C), which is a prerequisite to prevent internalization of pMHC molecules bound to the TCR, $t_{½}$ values can even be in the range of days (Supplementary Figure 1B and C). Although pMHC multimer dissociation experiments are capable of roughly distinguishing high and low avidity T cells within the same experiment, $t_{½}$ values and their differences underlie high inter-assay variability (Supplementary Figure 1B and C). Furthermore, the dissociation of multimeric complexes follows complicated rules: It is unclear how many monomeric MHC molecules are bound to a T cell and the number of MHC molecules per multimer is difficult to accurately determine.

To improve multimer-based $k_{off}$-rate measurements, we designed an assay to determine the dissociation kinetics of monomeric pMHC molecules from surface expressed TCRs (Fig. 1A) based on reversible *Strep*tamer stainings (17). Multiple pMHC molecules bind to *Strep*-Tactin via the *Strep*-tag sequences and stably label epitope-specific T cells (17, 18). The *Strep*tamer complex is disrupted by D-biotin. It binds to the *Strep*-tag binding sites on *Strep*-Tactin with higher affinity, leaving monomeric pMHC bound to surface expressed TCRs. By conjugating the pMHC molecules to a fluorescent dye, the dissociation kinetics of monomerized pMHCs can be observed as the decay in fluorescence intensity.

For fluorescence conjugation, a cysteine was inserted into the *Strep*-tag region and covalently linked to a dye carrying a maleimide group (Supplementary Fig. 2A). We found the bright and small Atto565 best suited for the setup, since it neither interferes with *Strep*-Tactin binding, nor with the binding of the pMHC to the TCR. Further, we replaced a cysteine with tyrosine at position 67 in the $\beta_2$-microglobulin, as this residue is solvent exposed, freely accessible (19), and allows dye conjugation of different MHC alleles within a conserved substructure. *Strep*tamers conjugated at both conjugation sites stained murine T cells and provided comparable $k_{off}$-rate data (Supplementary Fig. 2B). Fluorochrome conjugation to cysteine 67 in the $\beta_2$-microglobulin abrogated human *Strep*tamer stainings for different MHC alleles and peptide specificities. Therefore, all human $k_{off}$-rate data were exclusively obtained with the C-terminus Atto565 dye conjugation.

To prevent internalization of MHC molecules (17), *Strep*tamer-stained cells were constitutively kept at 4°C. Temperature control under the microscope was achieved by a customized cooling device connected to a peltier cooler. Cells were added into a buffer reservoir which fits exactly into the cooling device (Fig. 1B) and arrested by a polycarbonate membrane weighed down with a small metal shim to prevent movement (Fig. 1C and Supplementary movie S1). Fluorescence images were taken before and every 10 seconds after the addition of D-biotin until complete dissociation of the MHCs.

Fluorescence values were corrected for photobleaching (Supplementary Method 1). The photobleaching rate was monitored by analyzing *Strep*-Tactin coated beads multimerized with dye-conjugated MHC-molecules with identical settings (Fig. 1D, Supplementary Fig. 3 and Supplementary movie S2). Addition of D-biotin to Atto565-conjugated pMHCs multimerized on *Strep*-Tactin beads resulted in a quick loss of fluorescence, demonstrating no interference of the C-terminal dye-conjugation at the *Strep*-tag sequence with the *Strep*-Tactin binding or dissociation (Supplementary Fig. 4 and Supplementary movies S3 and S4).

### Analysis of individual T cells in the $k_{off}$-rate assay

Human CMV-specific T cells were purified from healthy blood donors PBMCs, stained with *Strep*-Tactin Allophycocyanin (APC, blue) and MHC Atto565 (red) double-labeled *Strep*tamers, and subsequently analyzed in the $k_{off}$-rate assay setup by real time fluorescence microscopy (Fig. 2A). Surprisingly, in the *Strep*tamer complex the MHC-Atto565 fluorescence intensity of stained cells was weak (Fig. 2A and B, 0s). After addition of D-biotin, *Strep*-Tactin APC dissociated and its fluorescence quickly decreased. In contrast, the quenched MHC-Atto565 fluorescence reached maximal intensity after *Strep*-Tactin-APC removal (Fig. 2B, 60 s), followed by a fluorescence decrease that reflects the dissociation of monomeric MHCs (Fig. 2B, 120 - 520 s and Supplementary movie 5 and 6). The maximal Atto565 fluorescence facilitated the $k_{off}$-rate analysis by identifying the starting point of the dissociation of monomeric MHC molecules. In contrast, simultaneous dissociation of MHC and *Strep*-Tactin during the first seconds after addition of D-biotin might complicate the analysis. Fluorescence intensities of individual cells were plotted over time and the $k_{off}$-rate and half-life time ($t_{½}$) of the binding was calculated as described in methods (Fig. 2C).

By using *Strep*-Tactin without fluorochrome conjugation we measured highly comparable $t_{½}$ of two T cell clones, indicating no influence of the APC on the Atto565 fluorescence decrease (Supplementary Fig. 5).

To compare the *Strep*tamer $k_{off}$-rate assay with conventional multimer dissociation experiments, we analyzed a number of T cell clones with both approaches. In the *Strep*tamer $k_{off}$-rate assay, T cell clone #1 had a mean $t_{½}$ of 200 seconds and clone #2 an approximately 4-fold shorter $t_{½}$ of 55 seconds (Supplementary Figure 6). Conventional multimer dissociation experiments using the same T cell clones determined very different values in two independent experiments (Supplementary Figure 1). In contrast, *Strep*tamer $k_{off}$-rate measurements of the T cell clones were much more reproducible, as shown in Fig.2D, Supplementary Figure 1 and 6 in different dissociations of two or three independent experiments. Furthermore, the *Strep*tamer $k_{off}$-rate assay was not influenced by pMHC rebinding, as off-rate kinetics were not different in the presence of antibodies blocking pMHC rebinding (Supplementary Figure 7). These data illustrate the specific advantages of the monomeric *Strep*tamer $k_{off}$-rate assay over conventional pMHC multimer dissociation experiments.

Next, we compared the $k_{off}$-rate assay to published data on TCR affinity by analyzing well characterized 2C TCR transgenic cells that recognize the allogeneic ligand H2-$L^d$/p2Ca and the syngeneic ligands H2-$K^b$/dEV8 and H2-$K^b$/SIY. Similar to results determined by SPR (20), we calculated higher $t_{½}$ for the 2C TCR/H2-$K^b$/SIY complex (mean $t_{½}$ 64.7 s) as compared to the TCR/H2-$K^b$/dEV8 with a mean $t_{½}$ of 12.7 s (Fig. 2E).

Taken together, we established an assay that provides reproducible data on MHC $k_{off}$-rates that are comparable for 2C ligands to those determined by SPR.

## Correlation between functional avidity and $k_{off}$-rate of two CMV-specific T cell clones

To analyze the correlation between $k_{off}$-rate values and functional avidity of T cells, we analyzed two human T cell clones specific for different epitopes derived from human CMV Immediate Early 1 antigen (IE1) (Fig. 3A). HLA-B8/$IE1_{88\text{-}96}$-specific clone B had a longer $t_{½}$ (mean = 178.3 s) compared to HLA-B8/$IE1_{199\text{-}207K}$-specific clone A (mean $t_{½}$ = 40.6 s) (Fig. 3B). In a chromium-release-assay and intracellular cytokine-staining, clone B reached half-maximal specific lysis of peptide pulsed target cells and half-maximal IFNγ production ($EC_{50}$) at lower peptide concentrations in comparison to clone A (Fig. 3C and D). Functional avidity of the clones correlated well with the differences determined by the $k_{off}$-rate assay.

TCRs from both clones A and B were isolated, expressed on $CD8\alpha^+$ Jurkat cells and analyzed in the $k_{off}$-rate assay (Table S1, Fig. 3E). Highly comparable $t_{½}$ of T cell clones and transduced Jurkat cells demonstrate that the TCR is the main determinant of measured $k_{off}$-rates (Fig. 3F).

## $k_{off}$-rates of CMV-specific T cell populations derived from different individuals

Enriched CMV-reactive T cells are a promising source for adoptive immunotherapy, and T cell avidity might be a relevant parameter to guide the selection of protective donor cells.

Therefore, we performed *ex vivo* $k_{off}$-rate analyses on four CMV-specific T cell populations derived from three different individuals and found strong variances in $k_{off}$-rates between individual populations (Fig. 4A). For further validation of the $k_{off}$-rate assay, we analyzed T cell clones derived from each of these populations. Indeed, with rare exceptions, the $t_{½}$ of the clones was in the range of values obtained from the respective CMV-specific T cell populations (Fig. 4 B-E; range indicated by dashed line or Table S2-5). We found only two clones with a shorter $t_{½}$ than its originating HLA-B8/$IE1_{88-96}$-specific population, which may have been missed in the *ex vivo* measurement. Sequencing analysis identified identical TCR sequences for the two 'outlier' clones with very similar $t_{½}$, emphasizing the high reproducibility of the $k_{off}$-rate assay and its independence of the cellular context. For two TCR identical T cell clones #1 and #2, we compared their $k_{off}$-rates measured early after T cell restimulation ("d12") and in a resting phase after restimulation ("d21"). In both cases, we obtained very comparable $k_{off}$-rates of the T cell clones (Supplementary Figure 8), demonstrating that the results of the $k_{off}$-rate assay are not dependent on the activation status of the measured T cells.

We analyzed T cell populations of four further donors reactive against the same pMHC (HLA-B8/$IE1_{199-207K}$), and detected a high variance in the mean $t_{½}$. These data indicate – at least for this pMHC specificity - that neither the HLA restriction, nor the epitope recognition, is a major determinant for a distinct $k_{off}$-rate of CMV specific populations. Most importantly, the $k_{off}$-rate of these *ex vivo* populations correlated, with the functional avidity (Supplementary Figure 9).

In summary, by analyzing CMV-specific T cells we further confirmed the reliability and reproducibility of $k_{off}$ rate measurements with this novel assay. We discovered remarkable differences in $k_{off}$-rates values of different CMV-specific T cell populations, suggesting the potential for different protective capacity in immunotherapy.

## Correlation between $k_{off}$-rate and in vivo protectivity of T cells in preclinical mouse models

Having demonstrated a correlation between the functional avidity and the $t_{½}$ *in vitro*, we analyzed the correlation between the $t_{½}$ and *in vivo* functionality of T cells. We generated polyclonal T cell lines A and B specific for the *Listeria monocytogenes* epitope $LLO_{91-99}$ by *in vitro* restimulation with high ($10^{-6}$ M) and low ($10^{-9}$ M) peptide concentrations. In line with published data (21), high peptide concentration expanded low avidity T cell line A that required higher peptide concentrations for half-maximal specific lysis of target cells or half-maximal IFN$\gamma$ secretion in comparison to cell line B (Fig. 5A and B). In the $k_{off}$-rate assay most cells from cell line A had a short $t_{½}$ below 30 seconds, while cells from cell line B were more heterogeneous with 38 % having a high $t_{½}$ between 100 and 340 seconds (Fig. 5C). *In vivo* protectivity was tested by adoptively transferring cells from each population into BALB/c mice, infecting the mice with *L. monocytogenes*, and analyzing bacterial load in spleens and livers three days later. Mice that had received cell line A were not protected, as they had high bacterial loads in the spleen comparable to the PBS control group, whereas mice that had received cell line B demonstrated a >100-fold reduction of viable bacteria in the spleen (Fig. 5D).

Because of the clinical relevance of CMV-specific T cells for adoptive immunotherapy and the large spectrum of $k_{off}$-rates measured in different epitope-specific human T cell populations, we further tested the correlation of $k_{off}$-rate and protection in a mouse model for CMV infection. We generated cell line A ($10^{-8}$ M) and B ($10^{-10}$ M) with high and low concentrations of the murine CMV (MCMV) epitope $m164_{257\text{-}265}$. Similar to Listeria-specific T cell lines, cell line B showed a higher functional avidity determined by $^{51}Cr$ release and Elispot assays (Fig. 5E and 5F) that correlated with a high proportion of cells with long $t_{½}$ above 50 seconds (Fig. 5G). At day 11 after transfer of cells from cell line A or B into immunosuppressed and MCMV-infected BALB/c mice, the number of MCMV plaque forming units (PFU) was determined (Fig. 5H). Only mice that had received cells from cell line B showed a remarkable reduction (>100 fold) in virus titers compared to control mice and mice that received cell line A.

These data strongly support the interpretation that T cell lines comprised of cells with slow MHC binding $t_{½}$ are superior to protect mice from *L. monocytogenes* and MCMV infections in adoptive transfer experiments.

## Discussion

Although TCR avidity is believed to be an important component for *in vivo* T cell efficacy, this parameter is still difficult to determine. Therefore, the aim of this study was to develop a technology for precise acquisition of an important part of the structural avidity of the TCR, the $k_{off}$-rate. By combining reversible MHC multimer staining with real time microscopy, we succeed to quantitatively determine $k_{off}$-rates. Using this assay, we demonstrate that CMV-specific T cell populations with different epitope-specificities or derived from different donors vary substantially in their $k_{off}$-rates. Adoptive T cell transfer experiments using preclinical mouse models show that T cell lines containing cells with slow $k_{off}$-rates have a higher protective capacity *in vivo*.

Our new technology overcomes several technical difficulties of current methods used to determine the binding strength between pMHC and TCR. For example, the analysis of conventional MHC multimer-based $k_{off}$-rate assays (16) is complicated by multivalent binding and dissociation rates, whereas the MHC-Streptamers homogenizes the system to measure truly monomeric interactions (Fig. 1). This is best illustrated by the large differences in the values of $k_{off}$-rates, which are in the range of minutes to hours for conventional MHC multimers (Supplementary Fig. 1 and reviewed in (16)) and in the range of seconds to minutes for monomeric interactions – determined by SPR or our newly developed $k_{off}$-rate assay (Fig. 2E and Supplementary Fig. 6). In addition, conventional MHC multimer-based $k_{off}$-rate assays require a blocking reagent to prevent rebinding of dissociated MHC molecules, and quality parameters of these blocking reagents (e.g. affinity, concentration) can further influence the obtained dissociation kinetics. As a consequence, the kinetics of $k_{off}$-rates determined by conventional MHC multimers is influenced by various factors unrelated to monomeric TCR pMHC interactions making it difficult to compare results obtained with different T cell populations. In contrast, the monomeric *Strep*tamer $k_{off}$-rate assay does not depend on the addition of a blocking reagent

(Supplementary Fig. 7) and is highly reproducible over different experiments (Supplementary Fig. 6).

In order to determine to what extent results from the Streptamer-based $k_{off}$-rate assays compare to published data, we analyzed transgenic T cells expressing the 2C TCR (22), as this receptor has been well examined with SPR (20). For two cognate epitopes, dEV8 and SIY, which are both presented on H2-$K^b$, we measured a very similar difference in $k_{off}$-rates of TCR-bound pMHC compared to SPR results (Fig. 2E). The absolute values are slightly higher for $k_{off}$-rates determined by the reversible MHC multimer technology, but this can be explained by the contribution of CD8 co-receptor binding, which was not included in SPR measurements.

A limitation of the current design of the *Strep*tamer-based $k_{off}$-rate assay is that it cannot segregate TCR from CD8 co-receptor binding. However, this might be possible to overcome by the use of mutated MHC molecules that abolish CD8 binding to the alpha3 domain (23).

Our first direct *ex vivo* analyses on human CMV epitope-specific T cell populations demonstrate that cell populations with specificity to the same pathogen can differ substantially in the ligand binding strength of recruited TCRs (Fig. 4A and Supplementary Fig. 9). This is likely to be clinically important, as enriched CMV-reactive T cells are currently used for adoptive immunotherapy in immunocompromised patients (1, 2), in particular patients that have received allogeneic hematopoietic stem cell transplantation (HSCT). Surprisingly, the analysis of just a few CMV epitope-specific $CD8^+$ T cell populations revealed dramatic differences in clonal composition as well as $k_{off}$-rates of individual TCRs. Thereby, the largest CMV-specific T cell population analyzed in our study (HLA-B8/$IE1_{199\text{-}207K}$ from donor #1, Fig. 4) was characterized by a very short pMHC-binding half-life and low functional avidity, as determined *ex vivo* as well as on *in vitro* expanded T cell clones. We are currently performing several clinical trials on adoptive transfer of MHC *Strep*tamer-sorted CMV epitope-specific $CD8^+$ T cell populations for the treatment of therapy-resistant CMV disease upon allogeneic HSCT (EudraCT-Nr.: 2006-006146-34 and IMPACT- ClinicalTrials.gov Identifier: NCT01077908; first case reports of this promising approach have been recently published (1)). In this setting, we are planning a detailed analysis of $k_{off}$-rates for transferred donor T cell populations, which will allow correlation of this parameter with the therapeutic effects of immunotherapy. In the example presented in this report the largest CMV-reactive population was characterized by the lowest (functional and structural) avidity. There are other reports on low functional avidity of large CMV-specific $CD8^+$ T cell populations (24, 25), but whether these are exceptions or a common characteristic of the $CD8^+$ T cell response to CMV has to be determined. Based on the results from pre-clinical protection models (Fig. 5), we suggest that determining $k_{off}$-rates might help to select the most protective antigen-specific T cell populations for adoptive immunotherapy; thereby, the largest cell populations, which are easiest to detect and to purify, might not always be the best choice (26, 27).

In conclusion, we demonstrate that the development of a technology based on reversible MHC multimer staining provides reliable access to the $k_{off}$-rate of TCR-ligand interactions and a new parameter for measuring the quality of T cells. This parameter might not only be

useful to choose best suitable T cells for adoptive transfer, but also to assess the quality of induced or existing immunity, e.g. after vaccination or due to permanent exposition to antigen as in chronic infections or tumors.

## Materials and Methods

### Blood samples

Peripheral blood was obtained from healthy adult donors of both sexes. Written informed consent was obtained from the donors, and usage of the blood samples was approved according to national law by the local Institutional Review Board (Ethikkommission der Medizinischen Fakultät der Technischen Universität München) in accordance with the declaration of Helsinki. Three individuals were selected for in depth analysis of HCMV-specific T cell clones. No further randomization was used.

### Human T cell clones

Sort-purified *Strep*tamer$^{+}$ cells (HLA-B8/IE1$_{199\text{-}207K}$, HLA-B8/IE1$_{88\text{-}96}$, HLA-A2/pp65$_{495\text{-}503}$ or HLA-B7/pp65$_{417\text{-}426}$) from CMV$^{+}$ healthy donors were plated by limiting dilution (0.6 cells/well) and cocultured with 1*10$^{4}$ γ-irradiated allogeneic LCLs (50 Gy) and 7.5*10$^{4}$ PBMCs (35 Gy) in h-RP10$^{+}$ (RPMI 1640, 10 % human serum, 0.025 % L-Glutamine, 0.1 % HEPES, 0.001 % Gentamycin, 0.002 % Streptomycin, 0.002 % Penicillin) supplemented with anti-CD3 mAb (OKT-3, 30 ng/ml) and IL-2 (50 U/ml). 5*10$^{4}$ cells were restimulated every 14 days with 1*10$^{6}$ γ-irradiated allogenic LCLs and 5*10$^{6}$ PBMCs in h-RP+ supplemented with anti-CD3 mAb. IL-2 (50 U/ml) was added one day later. Cells were analyzed between days 10 - 21 after restimulation.

**Murine T cell lines—**LLO$_{91\text{-}99}$-specific T cells were isolated from spleens of BALB/c mice 7 days after *L. monocytogenes* infection and stimulated weekly by addition of 3*10$^{7}$ γ-irradiated (25 Gy) splenocytes of syngenic, naïve mice, loaded with the appropriate concentrations of LLO$_{91\text{-}99}$ peptide (10$^{-6}$ M and 10$^{-9}$ M) for 1 h. RP10$^{+}$ (RPMI 1640, 10 % FCS, 0.025 % L-Glutamine, 0.1 % HEPES, 0.001 % Gentamycin, 0.002 % Streptomycin, 0.002 % Penicillin) was supplemented with rat ConA supernatant (5 % T-Stim, inactivation of ConA by addition of 5 % α-MM) from the second *in vitro* restimulation.

MCMV-specific T-cell lines were generated and restimulated similarly with 10$^{-8}$ or 10$^{-10}$ M of the m164$_{257\text{-}265}$ peptide (27).

**TCR Transduction—**TCRs of the T cell clones were amplified by RACE-PCR and subsequently sequenced. The TCR transduction was performed as described (28). Briefly, TCR α- and β-chain were separately cloned in the retroviral vector MP71. Packaging was performed by triplasmid $CaCl_2$ transfection with the retroviral vector plasmid and the expression plasmids encoding the Moloney MLV *gag/pol* genes (pcDNA3.1MLV*g/p*, kindly provided by C. Baum, Hannover, Germany) and the MLV-10A1 *env* gene (pALF-10A1) (29) in Hek293T cells. Viral supernatant was spun down (800g) in Retronectin-coated 24 well plates together with Jurkat76 cells for 90 min at 32°C. Five days post transduction cells were analyzed for TCR expression by FACS.

**MHC class I molecules—**A cysteine on a glycine serine linker was inserted by site-directed mutagenesis into DNA-Vectors containing the respective MHC I molecule and the *Strep*-tag sequence. Vectors were expressed in *E. coli* strains and subsequently refolded with $\beta_2$-microglobuline at high dilution. Correctly folded MHC I molecules were purified by gel filtration (Superdex 200HR), pooled and incubated overnight in a buffer containing $NaN_3$, protease inhibitors (1 mM NaEDTA, Leupeptin, Pepstatin) and 0.1 mM DTT. The buffer was exchanged against PBS pH 7.3 to allow for conjugation with activated fluorescent dyes Alexa-488-maleimide or Atto565-maleimide in a molar ratio of 10:1 at RT for 2 h. Conjugated proteins were separated from unbound dye with gravity flow columns (illustra NAP-25 Column, GE-Healthcare), the buffer exchanged against PBS pH 8.0 containing $NaN_3$ and protease inhibitors (1 mM NaEDTA, Leupeptin, Pepstatin) and the protein stored in liquid nitrogen.

***Strep*tamer staining—**For MHC multimerization, 1 μg of Atto565 or Alexa488-conjugated MHC I and 0.75 μg *Strep*-Tactin-APC or -PE (IBA) were incubated 45 min in 50 μl FACS buffer following manufacturer's instructions. Cells were rested 30 min on ice before staining and antibodies were added for the last 20 min of the staining.

**Bulk analysis of T cell receptor avidity—**All $k_{off}$-rate assays were performed on a Zeiss LSM 510 or a Leica SP5 confocal laser scanning microscope. Cells were concentrated to $1*10^4$/μl, and 1 μl of cells was pipetted into the cooling reservoir as described. To test the influence of a MHC blocking antibody in our system, the $k_{off}$-rate measurements were performed similarly, but in the presence of 10μM W6/32 antibody added in combination with D-Biotin.

**Data analysis—**Images were analyzed using MetaMorph Offline image analysis software (Molecular Devices). Integrated fluorescence intensity inside a gate containing an individual cell was measured over the whole time series acquired. The identical gate in close proximity to the cell, but not containing a cell, was acquired for measurement of background fluorescence intensity. Data were logged into Microsoft Excel . With the analyzer software "analyzer.nt", the background correction of the fluorescence intensity and the plotting of the corrected values over time are carried out in an automated manner. To ensure optimal fitting of the data points to an exponential curve (Supplementary Method 1), the software allows for the adaption of the area of data points included for fitting by specifying the first and last valid data point. Thereby, fitting of each cell is controlled directly and incorrect fittings, e.g. due to variations at the end of the assay, can be avoided.

**Photobleaching measurements—**1 μg of either pMHC-I molecules conjugated to Alexa488 or Atto565 or biotinylated APC or PE were multimerized with 7 μl of *Strep*-Tactin agarose beads (Superflow, 50 % suspension, IBA) in a total volume of 50 μl for 45 min. Beads were washed and analyzed for fluorescence decay under the microscope with the same setup and settings used for cells (pictures = 200). Photobleaching values were obtained from the exponent of an exponential decay fitting curve of the background-corrected raw data and used for correction of the $k_{off}$-rate data (Supplementary Method 1).

**Conventional multimer dissociation experiment—**T cell clones were analyzed according to (16). Briefly, T cell clones were rested 30 minutes on ice before staining with conventional biotinylated HLA-B8/IE1$_{88-96}$ multimer PE for 45 minutes. After washing, cells were resuspended in 200μL FACS in the presence or absence of 10μM W6/32 blocking antibody (anti-HLA-A,B,C). Cells were kept at 4°C for 10h and aliquots were taken at the indicated time points. The maximal MFI of living multimer PE$^+$ was normalized to 100% and the normalized data plotted over the time. An exponential decay was fitted into the data and used to calculate the $t_{½}$.

**Intracellular cytokine staining—**T cells were incubated in the presence of the indicated amount of the respective peptides for 5 h in RP10$^+$ supplemented with anti-CD28 and anti-CD49d (BD Biosciences). 2 μg/well Brefeldin-A (Sigma) was added after 1 h (human cells) or 2 h (murine cells). After stimulation cells were kept at 4°C and stained with EMA (0.1 μg in 50 μl FACS buffer) for 20 min under light. For surface staining, cells were incubated 20 min in the dark with anti-CD8α mAb before lysis in Cytofix/Cytoperm (BD Biosciences) for 20 min and intracellular staining against IFN-γ (30 min, in the dark, on ice in BD Bioscience Perm/Wash buffer). The maximal percentage of IFNγ$^+$ CD8$^+$ was normalized to 100% and a nonlinear curve was fitted into the normalized data in response to each peptide concentration.

For CMV-specific T cell populations, 2*10$^6$ PBMCs from different donors were incubated per sample. Human T cell clones were cocultured with HLA/B8-expressing LCLs at an effector to target ratio of 10:1 and murine LLO$_{91-99}$-specific T cell lines with P815 cells at an effector to target ratio of 1:1.

**IFN-γ-based ELISPOT assay—**Titrated numbers of m164-specific T cells (50, 100 and 200) were stimulated for 18 h with 1*10$^5$ P815 cells that were loaded for 1 h at 37°C with the indicated concentrations of m164 peptide as described previously (30). All titration steps were performed in triplicates. Thereafter, plates were developed, spot numbers were counted and the frequencies of IFN-γ secreting spot-forming cells with the corresponding 95% confidence intervals were calculated by intercept-free linear regression analysis.

**$^{51}$Chromium release assay—**For the analysis of human T cell clones, 1*10$^6$ HLA/B8-expressing LCLs were loaded with the indicated amounts of IE1$_{88-96}$ or IE1$_{199-207K}$ peptide ($10^{-11}$ to $10^{-5}$ M) and 1.85 MBq $^{51}$Cr for 1 h at 37°C and $10^4$ cells used as target cells for 1*10$^5$ T cell clones (E/T-ratio = 10:1). To determine the spontaneous and maximal lysis, RP10$^+$ or 5 % Triton X-100 were used, respectively, instead of effector cells. All titration steps were performed in triplicates. The cells were incubated for 4-5 h at 37°C, spun down and the supernatants transferred to counting tubes. The amount of radioactivity in the supernatants was measured in a γ-counter and the specific lysis for each sample was calculated.

To test murine LLO$_{91-99}$- and m164$_{257-265}$- specific T cell lines, P815 target cells were labeled with 18.5 MBq $^{51}$Cr for 1 h at 37°C and loaded with their respective peptide in concentrations of $10^{-6}$ M to $10^{-13}$ M (LLO$_{91-99}$) or $10^{-6}$ M to $10^{-13}$ M (m164$_{257-265}$). Effector cells were co-cultivated and analyzed in an E/T-ratio of 10:1 as described above.

**Infection and adoptive cell transfer—**For *Listeria monocytogenes* infection of BALB/c mice, the isolate *L. monocytogenes* 10403s (ATCC) was used. Mice were infected intravenously (i.v.) with $2*10^4$ CFU of bacteria in 200 μl PBS 1 h after i.v. transfer of $5*10^6$ $LLO_{91-99}$-specific T cells. The organs were harvested at day 3 after infection, homogenized and resuspended in 5 ml sterile PBS. A serial dilution of the cells in 0.1% Triton X-100 was plated out on BHI plates and the CFU were counted after one night of incubation at 37°C.

For the MCMV protection assay (26, 27, 30), $10^6$ cells from the indicated cell line were transferred i.v. into 8- to 10-week-old female BALB/c recipients which were immunocompromised by total-body γ-irradiation with a single dose of 6.5 Gy before transfer. Subsequently, subcutaneous, intraplantar infection was performed at the left hind footpad with $10^5$ PFU of cell culture-propagated and then purified MCMV, strain Smith (ATCC VR-194/1981) in 25 μl of physiological saline. Infectious virus was quantitated on day 11 after transfer in homogenates of spleens by a virus plaque assay under conditions of centrifugal enhancement of infectivity.

## Supplementary Material

Refer to Web version on PubMed Central for supplementary material.

## Acknowledgments

We wish to express special thanks for support in performing experiments to Lotta Räty, Lydia Frimmer and Anna Hochholzer, for support in the development of analyzer software used for automated fitting of fluorescence data to Jörg Mages and Sebastian Nauerth, for flow cytometry-based cell sorting to Lynette Henkel, Matthias Schiemann, Immanuel Andrä and Katleen Wild, and for critical discussion of the manuscript to Patricia Gräf, Christian Stemberger and Veit Buchholz.

**Funding**

This work was supported by the SFB TR36 (TP-B10/13), SFB 1054 (TP-B09), SFB 490 (TP-E3) and a DFG grant from the Clinical Research Group KFO 183, individual project TP8.

## References and notes

1. Schmitt A, Tonn T, Busch DH, Grigoleit GU, Einsele H, Odendahl M, Germeroth L, Ringhoffer M, Ringhoffer S, Wiesneth M, Greiner J, Michel D, Mertens T, Rojewski M, Marx M, von Harsdorf S, Dohner H, Seifried E, Bunjes D, Schmitt M. Adoptive transfer and selective reconstitution of streptamer-selected cytomegalovirus-specific CD8+ T cells leads to virus clearance in patients after allogeneic peripheral blood stem cell transplantation. Transfusion. 2011; 51:591–599. [PubMed: 21133926]
2. Walter EA, Greenberg PD, Gilbert MJ, Finch RJ, Watanabe KS, Thomas ED, Riddell SR. Reconstitution of cellular immunity against cytomegalovirus in recipients of allogeneic bone marrow by transfer of T-cell clones from the donor. N Engl J Med. 1995; 333:1038–1044. [PubMed: 7675046]
3. Dudley ME, Wunderlich JR, Robbins PF, Yang JC, Hwu P, Schwartzentruber DJ, Topalian SL, Sherry R, Restifo NP, Hubicki AM, Robinson MR, Raffeld M, Duray P, Seipp CA, Rogers-Freezer L, Morton KE, Mavroukakis SA, White DE, Rosenberg SA. Cancer regression and autoimmunity in patients after clonal repopulation with antitumor lymphocytes. Science. 2002; 298:850–854. [PubMed: 12242449]
4. Dudley ME, Wunderlich JR, Yang JC, Sherry RM, Topalian SL, Restifo NP, Royal RE, Kammula U, White DE, Mavroukakis SA, Rogers LJ, Gracia GJ, Jones SA, Mangiameli DP, Pelletier MM, Gea-Banacloche J, Robinson MR, Berman DM, Filie AC, Abati A, Rosenberg SA. Adoptive cell

transfer therapy following non-myeloablative but lymphodepleting chemotherapy for the treatment of patients with refractory metastatic melanoma. J Clin Oncol. 2005; 23:2346–2357. [PubMed: 15800326]

5. Kolb HJ, Schattenberg A, Goldman JM, Hertenstein B, Jacobsen N, Arcese W, Ljungman P, Ferrant A, Verdonck L, Niederwieser D, van Rhee F, Mittermueller J, de Witte T, Holler E, Ansari H. Graft-versus-leukemia effect of donor lymphocyte transfusions in marrow grafted patients. Blood. 1995; 86:2041–2050. [PubMed: 7655033]
6. Derby M, Alexander-Miller M, Tse R, Berzofsky J. High-avidity CTL exploit two complementary mechanisms to provide better protection against viral infection than low-avidity CTL. J Immunol. 2001; 166:1690–1697. [PubMed: 11160212]
7. Dutoit V, Rubio-Godoy V, Dietrich PY, Quiqueres AL, Schnuriger V, Rimoldi D, Lienard D, Speiser D, Guillaume P, Batard P, Cerottini JC, Romero P, Valmori D. Heterogeneous T-cell response to MAGE-A10(254-262): high avidity-specific cytolytic T lymphocytes show superior antitumor activity. Cancer Res. 2001; 61:5850–5856. [PubMed: 11479225]
8. Zeh HJ, Perry-Lalley D, Dudley ME, Rosenberg SA, Yang JC. High avidity CTLs for two self-antigens demonstrate superior in vitro and in vivo antitumor efficacy. J Immunol (3rd). 1999; 162:989–994. [PubMed: 9916724]
9. Clay TM, Custer MC, Sachs J, Hwu P, Rosenberg SA, Nishimura MI. Efficient transfer of a tumor antigen-reactive TCR to human peripheral blood lymphocytes confers anti-tumor reactivity. J Immunol. 1999; 163:507–513. [PubMed: 10384155]
10. Morgan RA, Dudley ME, Yu YY, Zheng Z, Robbins PF, Theoret MR, Wunderlich JR, Hughes MS, Restifo NP, Rosenberg SA. High efficiency TCR gene transfer into primary human lymphocytes affords avid recognition of melanoma tumor antigen glycoprotein 100 and does not alter the recognition of autologous melanoma antigens. J Immunol. 2003; 171:3287–3295. [PubMed: 12960359]
11. Zhao Y, Zheng Z, Robbins PF, Khong HT, Rosenberg SA, Morgan RA. Primary human lymphocytes transduced with NY-ESO-1 antigen-specific TCR genes recognize and kill diverse human tumor cell lines. J Immunol. 2005; 174:4415–4423. [PubMed: 15778407]
12. Wilde S, Sommermeyer D, Frankenberger B, Schiemann M, Milosevic S, Spranger S, Pohla H, Uckert W, Busch DH, Schendel DJ. Dendritic cells pulsed with RNA encoding allogeneic MHC and antigen induce T cells with superior antitumor activity and higher TCR functional avidity. Blood. 2009; 114:2131–2139. [PubMed: 19587379]
13. Johnson LA, Heemskerk B, Powell DJ Jr. Cohen CJ, Morgan RA, Dudley ME, Robbins PF, Rosenberg SA. Gene transfer of tumor-reactive TCR confers both high avidity and tumor reactivity to nonreactive peripheral blood mononuclear cells and tumor-infiltrating lymphocytes. J Immunol. 2006; 177:6548–6559. [PubMed: 17056587]
14. Busch DH, Pamer EG. T cell affinity maturation by selective expansion during infection. J Exp Med. 1999; 189:701–710. [PubMed: 9989985]
15. Lyons DS, Lieberman SA, Hampl J, Boniface JJ, Chien Y, Berg LJ, Davis MM. A TCR binds to antagonist ligands with lower affinities and faster dissociation rates than to agonists. Immunity. 1996; 5:53–61. [PubMed: 8758894]
16. Wang XL, Altman JD. Caveats in the design of MHC class I tetramer/antigen-specific T lymphocytes dissociation assays. J Immunol Methods. 2003; 280:25–35. [PubMed: 12972185]
17. Knabel M, Franz TJ, Schiemann M, Wulf A, Villmow B, Schmidt B, Bernhard H, Wagner H, Busch DH. Reversible MHC multimer staining for functional isolation of T-cell populations and effective adoptive transfer. Nat Med. 2002; 8:631–637. [PubMed: 12042816]
18. Altman JD, Moss PA, Goulder PJ, Barouch DH, McHeyzer-Williams MG, Bell JI, McMichael AJ, Davis MM. Phenotypic analysis of antigen-specific T lymphocytes. Science. 1996; 274:94–96. [PubMed: 8810254]
19. Walter JB, Garboczi DN, Fan QR, Zhou X, Walker BD, Eisen HN. A mutant human beta2-microglobulin can be used to generate diverse multimeric class I peptide complexes as specific probes for T cell receptors. J Immunol Methods. 1998; 214:41–50. [PubMed: 9692857]
20. Garcia KC, Tallquist MD, Pease LR, Brunmark A, Scott CA, Degano M, Stura EA, Peterson PA, Wilson IA, Teyton L. Alphabeta T cell receptor interactions with syngeneic and allogeneic

ligands: affinity measurements and crystallization. Proc Natl Acad Sci U S A. 1997; 94:13838–13843. [PubMed: 9391114]

21. Alexander-Miller MA, Leggatt GR, Berzofsky JA. Selective expansion of high- or low-avidity cytotoxic T lymphocytes and efficacy for adoptive immunotherapy. Proc Natl Acad Sci U S A. 1996; 93:4102–4107. [PubMed: 8633023]
22. Kranz DM, Sherman DH, Sitkovsky MV, Pasternack MS, Eisen HN. Immunoprecipitation of cell surface structures of cloned cytotoxic T lymphocytes by clone-specific antisera. Proc Natl Acad Sci U S A. 1984; 81:573–577. [PubMed: 6607474]
23. Purbhoo MA, Boulter JM, Price DA, Vuidepot AL, Hourigan CS, Dunbar PR, Olson K, Dawson SJ, Phillips RE, Jakobsen BK, Bell JI, Sewell AK. The human CD8 coreceptor effects cytotoxic T cell activation and antigen sensitivity primarily by mediating complete phosphorylation of the T cell receptor zeta chain. J Biol Chem. 2001; 276:32786–32792. [PubMed: 11438524]
24. Ouyang Q, Wagner WM, Wikby A, Walter S, Aubert G, Dodi AI, Travers P, Pawelec G. Large numbers of dysfunctional CD8+ T lymphocytes bearing receptors for a single dominant CMV epitope in the very old. J Clin Immunol. 2003; 23:247–257. [PubMed: 12959217]
25. Hadrup SR, Strindhall J, Kollgaard T, Seremet T, Johansson B, Pawelec G, thor Straten P, Wikby A. Longitudinal studies of clonally expanded CD8 T cells reveal a repertoire shrinkage predicting mortality and an increased number of dysfunctional cytomegalovirus-specific T cells in the very elderly. J Immunol. 2006; 176:2645–2653. [PubMed: 16456027]
26. Holtappels R, Simon CO, Munks MW, Thomas D, Deegen P, Kuehnapfel B, Daeubner T, Emde SF, Podlech J, Grzimek NK, Oehrlein-Karpi SA, Hill AB, Reddehase MJ. Subdominant CD8 T-cell epitopes account for protection against cytomegalovirus independent of immunodomination. J Virol. 2008; 82:5781–5796. [PubMed: 18367531]
27. Ebert S, Podlech J, Gillert-Marien D, Gergely KM, Buettner JK, Fink A, Freitag K, Thomas D, Reddehase MJ, Holtappels R. Parameters determining the efficacy of adoptive CD8 T-cell therapy of cytomegalovirus infection. Med Microbiol Immunol. 2012; 201:527–539. [PubMed: 22972232]
28. Engels B, Cam H, Schuler T, Indraccolo S, Gladow M, Baum C, Blankenstein T, Uckert W. Retroviral vectors for high-level transgene expression in T lymphocytes. Hum Gene Ther. 2003; 14:1155–1168. [PubMed: 12908967]
29. Uckert W, Becker C, Gladow M, Klein D, Kammertoens T, Pedersen L, Blankenstein T. Efficient gene transfer into primary human CD8+ T lymphocytes by MuLV-10A1 retrovirus pseudotype. Hum Gene Ther. 2000; 11:1005–1014. [PubMed: 10811229]
30. Holtappels R, Thomas D, Podlech J, Reddehase MJ. Two antigenic peptides from genes m123 and m164 of murine cytomegalovirus quantitatively dominate CD8 T-cell memory in the H-2d haplotype. J Virol. 2002; 76:151–164. [PubMed: 11739681]

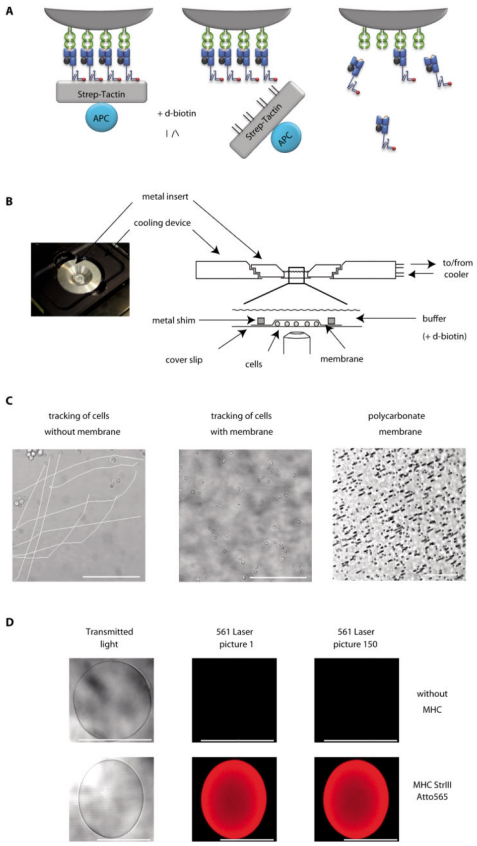


**Figure 1. Basic principle and experimental realization of the $k_{off}$-rate assay**

(**A**) Specific $CD8^+$ T cells are stably labeled with dichromatic *Strep*tamers (left). Addition of D-biotin displaces *Strep*-Tactin, leaving monomeric pMHC molecules bound to surface expressed TCRs (middle). Subsequent dissociation of monomeric MHC molecules is observed as a decay of the Atto565 fluorescence by real-time microscopy. (**B**) A cooling device is mounted on the microscope (left). Purified T cells are pipetted into a 4°C cooled reservoir build of a metal insert sealed with a cover slip, arrested by a polycarbonate membrane and a metal shim and covered with cold buffer (right). (**C**) Reduced movement of cells covered with polycarbonate membrane (middle) in comparison to cells not arrested (left) over a time series of 200 pictures after addition of D-biotin. 5μm pores in the membrane allow quick diffusion of buffer (right, dark spots). (**D**) Validation of Atto565 fluorescence on agarose *Strep*-Tactin beads in the $k_{off}$-rate setup. Transmitted light and Atto565 fluorescence of unloaded beads (upper row) or beads loaded with Atto565 labeled MHC molecules (lower row) of two representative experiments. Scale bars indicate 100μm.

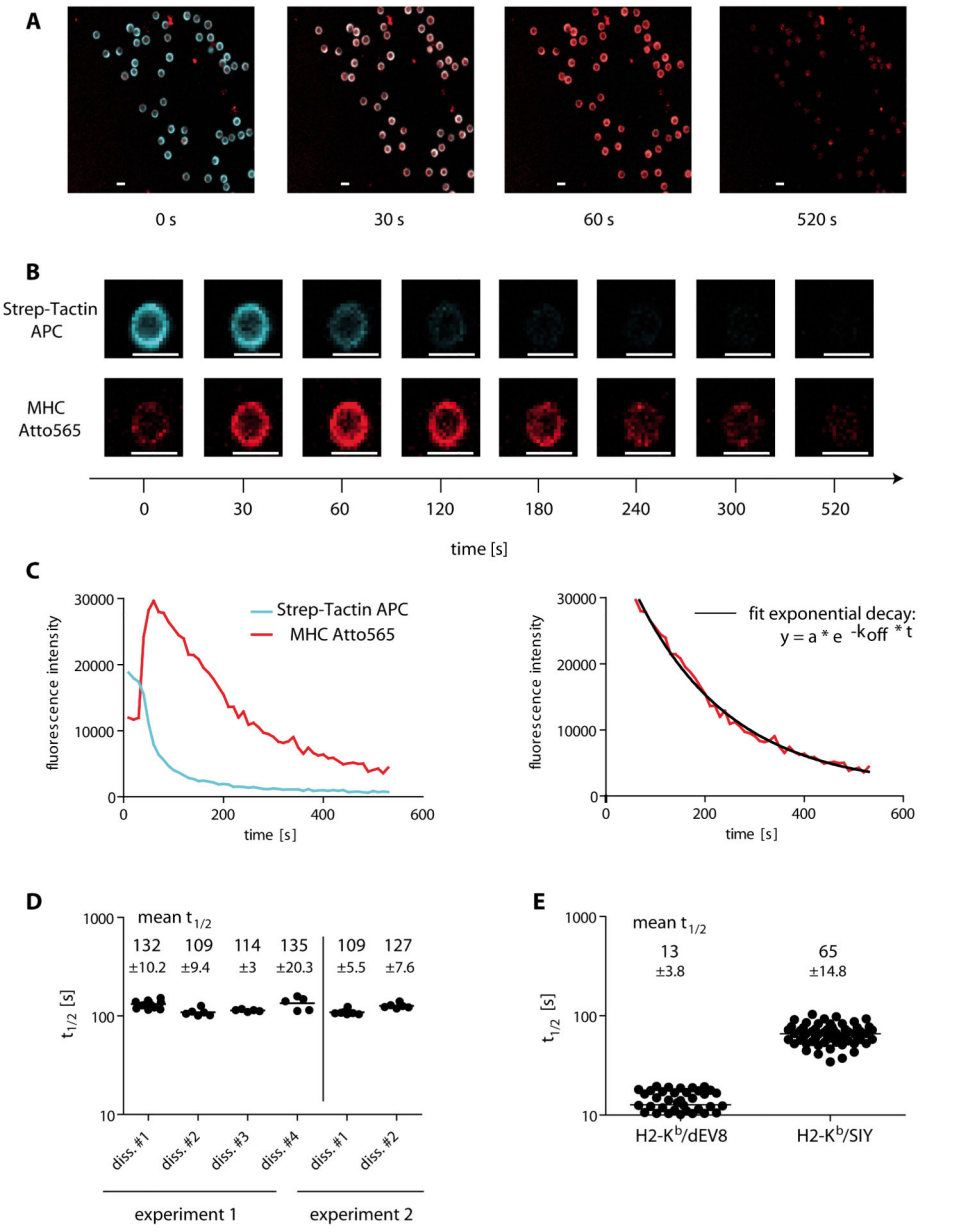


**Figure 2. Analysis of individual antigen-specific T cells in the monomeric *Strep*tamer $k_{off}$-rate assay**

(**A**) Overlay of the Allophycocyanin (APC) and the Atto565 fluorescence of *Strep*tamer stained and FACS-sorted HLA-B7/pp65$_{417-426}$-specific human T cells before (0s), and at 30s, 60s and 520s after the addition of D-biotin. (**B**) Gating on a single cell derived from the images shown in (**A**) with separated pictures for APC (upper row) and Atto565 fluorescence (lower row). The scale indicates the time after addition of D-biotin and scale bars indicate 10 μm. (**C**) Plot of the fluorescence intensity of APC (blue line) and Atto565 (red line) over time after the addition of D-biotin (left). Fit of a curve with exponential decay into the data points after maximum fluorescence of Atto565 (right). (**D**) Reproducibility of the analyzed data in different dissociations and independent experiments. The graph shows the $t_{½}$ of a human T cell clone in 6 individual dissociations of two independent experiments. Numbers

in the graph indicate the mean $t_{½}$ with standard deviation (±SD) for each measurement. (**E**) $k_{off}$-rate assay of 2C T cells. The $t_{½}$ of 51 and 60 single cells stained with H2-Kb/dEV8 or H2-Kb/SIY *Strep*tamers, respectively, each from four independent dissociations are plotted with the mean ±SD.

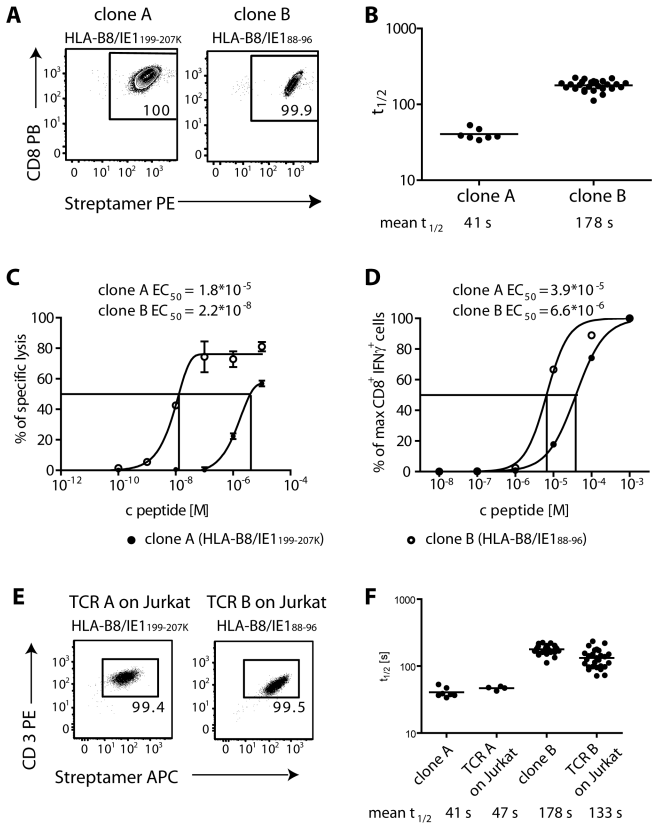


**Figure 3. $k_{off}$-rate of two human T cell clones is maintained after transgenic expression of TCRs in Jurkat76 cells**

(**A**) *Strep*tamer-staining of T cell clones A (specific for HLA-B8/IE1$_{88-96}$) and clone B (specific for HLA-B8/IE1$_{199-207K}$). FACS dot plots show CD8 vs. *Strep*tamer-staining, cells are pre-gated on living cells. (**B**) $k_{off}$-rate assay of clone A and clone B. The $t_{½}$ of 7 and 26 single cells from clone A and B, respectively, each from two independent dissociations are plotted with the mean ±SD. (**C**) 1*10$^5$ cells from T cell clones A and B were incubated at an E:T ratio of 10:1 with target cells from a HLA/B8-expressing lymphoblastoid cell line (LCL), which were labeled with $^{51}$Cr and loaded with the indicated amount of IE1$_{199-207K}$ or IE1$_{88-96}$ peptide, respectively. Lysis of target cells was measured in a γ-counter as the amount of radioactivity released into the culture supernatant in triplicates. The peptide concentration for the half maximal lysis ($EC_{50}$) was calculated by fitting a non-linear regression curve. (**D**) 1*10$^6$ T cells and 1*10$^5$ HLA/B8-expressing LCLs were incubated with the indicated amounts of IE1$_{199-207K}$ or IE1$_{88-96}$ peptide, respectively, and IFNγ production was analyzed by ICCS. The percentage of CD8$^+$ IFNγ$^+$ living cells was normalized to the maximum and peptide concentration for half maximal IFNγ production ($EC_{50}$) was calculated after fitting a non-linear regression curve. (**E**) *Strep*tamer-staining of Jurkat76 cells expressing the TCRs of clone A and clone B, respectively. Dot plots show CD3 vs. *Strep*tamer-staining, gated on living cells. (**F**) Comparison of the $k_{off}$-rate data of clone A and B from (**B**) to $t_{½}$ of 4 and 27 single cells from Jurkat76 cells transduced with the identical TCR A and B from three and six independent dissociations with the mean $t_{½}$, respectively.

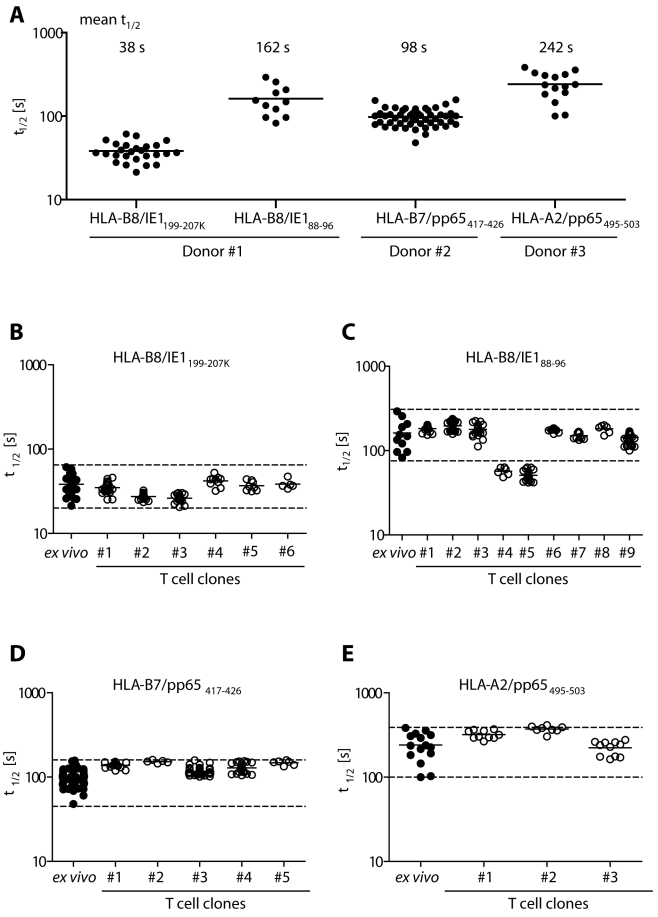


**Figure 4. $k_{off}$ rates of polyclonal *ex vivo* CMV-specific T cell populations show remarkable variability and define the range for the $t_{½}$ of their respective clones.**

(**A**) TCR $k_{off}$-rates ($t_{½}$) of four individual CMV-specific $CD8^+$ T cell populations from three different donors sorted by flow cytometry from purified PBMCs after staining with αCD8 antibody and *Strep*tamers. The $t_{½}$ of 26, 11, 50 or 15 individual cells of HLA-B8/$IE1_{199-207K,}$ HLA-B8/$IE1_{88-96}$, HLA-B7/$pp65_{417-426}$ and HLA-A2/$pp65_{495-503}$ specific T cells, respectively, each from two or six independent dissociations for HLA-B8/$IE1_{88-96}$ are plotted with its mean. (**B–E**) T cell clones were grown from flow cytometry sorted CMV-specific *ex vivo* populations by limiting dilution. $t_{½}$ of the *ex vivo* populations and their respective clones (specificity indicated at the top of the diagram) are compared. Mean $t_{½}$ values and number of analyzed cells are summarized in Table S2 - S5.

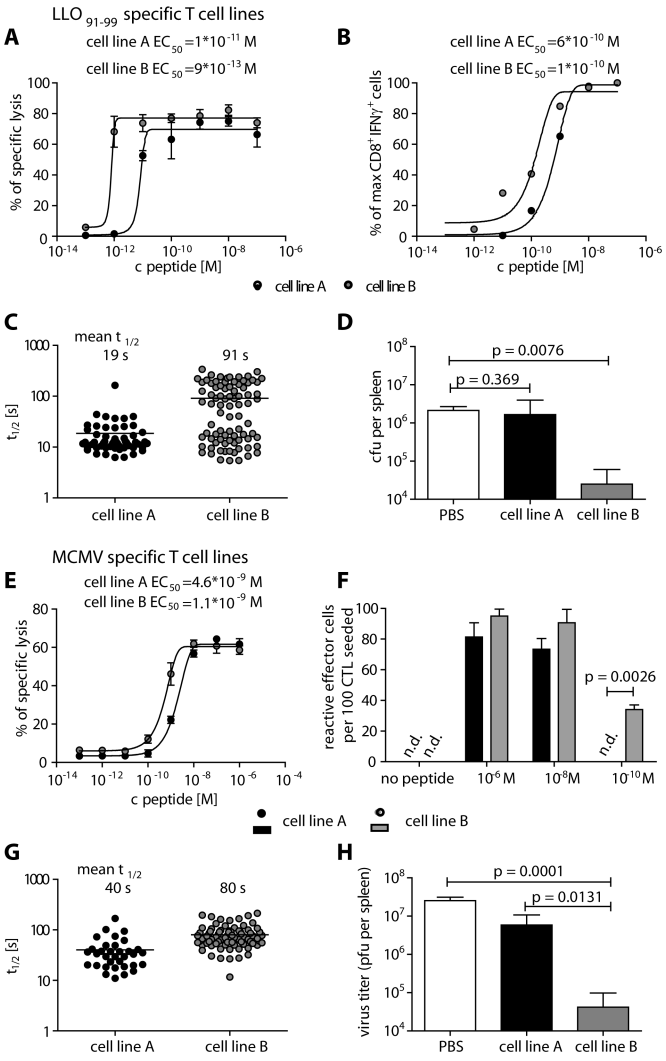


**Figure 5. Long t½ correlates with high functional avidity and protectivity of T cell lines in *L. monocytogenes* and MCMV infection**

(**A-D**) $LLO_{91-99}$-specific T cells restimulated with $10^{-6}$ M (cell line A) or $10^{-9}$ M peptide (cell line B). (**A**) Specific killing of $LLO_{91-99}$-specific T cell lines was tested in a chromium release assay by incubation with $^{51}Cr$ labeled and peptide loaded P815 target cells at an E:T ratio of 10:1 in triplicates. The peptide concentration for the half maximal lysis ($EC_{50}$) was calculated after fitting a non-linear regression curve. (**B**) IFNγ production of $LLO_{91-99}$-specific T cell lines was analyzed by ICCS after incubation with P815 target cells and the indicated amounts of peptide at an E:T ratio of 1:1. Values were normalized to maximal IFNγ production and the $EC_{50}$ was calculated after non-linear regression. (**C**) $k_{off}$-rate assay of $LLO_{91-99}$ -specific T cell lines A and B. The t½ of 54 or 84 individual cells of cell line A or B, respectively, each from three independent dissociations are plotted with the mean±SD. (**D**) Bacterial load of mice transferred with PBS or $5*10^6$ cells from $LLO_{91-99}$ -specific cell line A or B 3 days after *L. monocytogenes* infection ($2*10^4$ CFU) (n=3). Groups were compared by one-tailed t-test. (**E-H**) $m164_{257-265}$ specific T cells restimulated with $10^{-8}$ M (cell line A) or $10^{-10}$ M (cell line B) peptide. (**E**) Specific killing of $m164_{257-265}$ -specific T

lines A and B was tested as described in the methods section. (**F**) IFN$\gamma$-production of $m164_{257\text{-}265}$ -specific T cell lines was tested in triplicates by ELISPOT after 18h incubation with peptide loaded P815 target cells and frequencies of spot-forming cells were calculated. (**G**) $k_{off}$-rate assay of $m164_{257\text{-}265}$ specific T cell lines. The $t_{½}$ of 34 or 78 individual cells from five independent dissociations of cell line A or B, respectively, are plotted. (**H**) Virus titer was quantitated 11 days after i.v. injection of PBS or $10^6$ cells from $m164_{257\text{-}265}$ specific T cell line A or B into immunocompromised, MCMV infected mice (n=6). Groups were compared by one-tailed t-test.